

CHAPTER 23

TRANSFORMATION OF IRREGULAR WAVES IN SHOALING WATER

Tetsuo Sakai
Assistant Professor
and
Yuichi Iwagaki
Professor
Department of Civil Engineering
Kyoto University
Kyoto, Japan

ABSTRACT

In the numerical method of prediction of wind waves in deep water, Hasselmann's nonlinear interaction theory is applied. This method assumes the energy balance of individual component waves. However, the total energy balance must exist in the transformation of irregular waves in shoaling water. In this investigation, experiments were carried out on the transformations in shoaling water of composite waves having two components and random waves having one or two main peaks.

It was found that the elementary component wave height of the composite waves and the elementary peak power of the random waves decrease with decrease in the water depth. This reason can be explained qualitatively by the theory of the elementary component wave height change of finite amplitude waves in shoaling water. The secondary component wave height of the composite waves and the secondary peak power of the random waves increase with decrease in the water depth. This can be explained qualitatively by Hamada's theory of nonlinear interaction in uniform depth.

INTRODUCTION

The mechanism of transformation in shoaling water of wind waves, swell, tsunami and so on is one of the elementary problems in coastal engineering. In fact, the action of waves on coastal and offshore structures is the most important factor in design of the structures in coastal and offshore zones. In this case, the accurate estimation of the transformation of waves predicted in deep water is required. In the traditional design, irregularity of waves in actual coasts has not been taken into account directly, and irregular waves have been represented by regular waves having a significant wave height and period. However, it is expected that phenomena inherent in irregular waves occur in some cases. Recently, irregularity of waves is taken into account directly in design.

On the transformation of irregular waves in shoaling water, there are some investigations which irregularity of waves is taken into account directly by the power spectral density representation. Bretschneider¹⁾ and Tang-Ou²⁾ discussed the transformation of irregular waves by assuming the independency of individual components. However, it is expected that the nonlinearity of waves becomes predominant near the breaking point and the assumption of independency of the components becomes unsuitable.

In general, Hasselmann's nonlinear interaction model³⁾ is used in the transformation of irregular waves in deep water. The validity of this model has been confirmed on the transformation of irregular waves in uniform depth⁴⁾.

However, in the case of the transformation of waves in decreasing depth, the total energy balance including the energy dissipations due to boundary friction and wave breaking must exist.

In this investigation, the transformations of composite waves and random waves having predominant peaks are discussed experimentally. It is tried to explain the transformations by the theory of shoaling of finite amplitude waves. In addition to the power spectral density, the frequency distributions of water level, crest height and wave height are also important to represent irregular waves. However, they are not discussed here. It should be noticed that the word "composite waves" means the waves consisting of finite number of sinusoidal waves and the word "random waves" means the waves consisting of infinite number of sinusoidal waves and determined only stochastically.

EXPERIMENTS ON TRANSFORMATION OF IRREGULAR WAVES IN SHOALING WATER

COMPOSITE WAVES

a) Experimental apparatus

A wave tank at the Department of Civil Engineering, Kyoto University was used. The length of the tank is 28m, the height 75cm and the width 50cm. A hydraulic composite wave generator of piston type is installed at one end of the tank (see Photo.1). This generator consists of 8 pistons⁵). The period ratio of one piston to the next piston is $1/\sqrt{2}$. The generator generates the composite waves by imposing these motions upon the wave board simultaneously.

As seen in Fig.1, a wave absorber was installed at the opposite end of the tank and a uniform sloping beach was set in the middle part of the tank. This beach was made of aluminium plates. The slope of the beach was 1/20. Its length was 7.2m and the height of the slope tail was 36cm. In the experiments, the water depth in the uniform depth region was kept constant (36cm). Therefore, waves after breaking flew over the beach tail. In this way, the wave reflection from the beach and wave setup and down were made to be negligible as much as possible.

One wave gauge was set in the uniform depth region and three on the beach. The water level variations at four measuring points were recorded simultaneously with a magnetic tape recorder. The positions of two wave gauges in the uniform depth region and at the deepest measuring point on the beach were fixed during the experiments (see Fig.1). The wave gauge in the shallowest measuring point on the beach was set at the breaking point of the composite waves. The breaking point of the composite waves was determined as the deepest one among the breaking points varying with time. Four measuring points were numbered as 1, 2, 3 and 4 in order from offshore.

b) Procedure of experiment and analysis

The composite waves were generated by using two pistons of the generator. Before the experiments of composite waves, the experiments of monochromatic waves using each one of these pistons were carried out. The period ratio of two pistons used was $1/\sqrt{2}$. The analog data in the magnetic tape recorder were converted into the digital data (the time increment was 0.08sec) with a A-D convertor. The experimental conditions are shown in Table 1.

The monochromatic waves consist of one elementary component and the harmonic components. In so far as the nonlinear interaction of 2nd order, the harmonic component is only the component of two times the elementary component frequency.

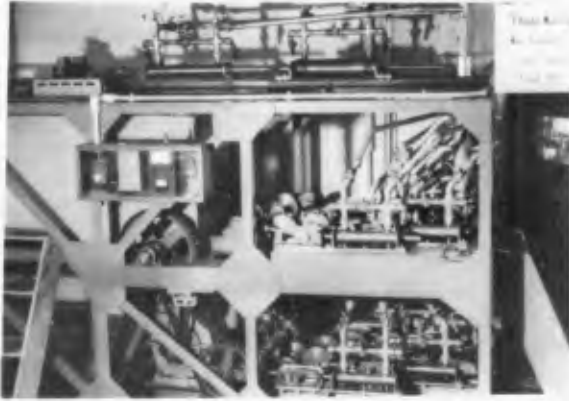


Photo.1 Composite wave generator

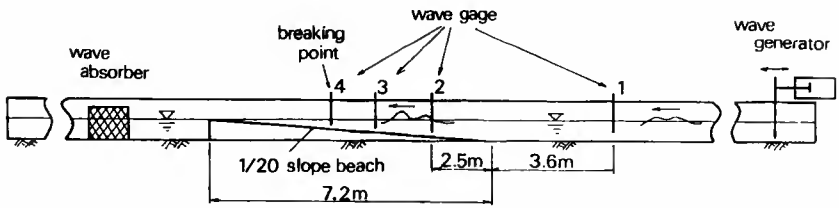


Fig.1 Experimental apparatus(composite waves)

Table 1 Experimental conditions (composite waves)

Run No.	Wave period	Water depth				Wave height at h_1
		Gauge No.1 uniform depth	No.2	No.3	No.4	
		h_1 (cm)	h_2 (cm)	h_3 (cm)	h_4 (cm)	
1	1.00	36.0	23.5	14.3	6.0	1.2
2	0.71	36.0	23.5	14.3	6.0	1.8
3		36.0	23.5	14.3	6.0	
4		36.0	23.5	14.7	8.8	2.0
5	0.85	36.0	23.5	14.7	8.8	3.0
6		36.0	23.5	14.7	8.8	
7		36.0	23.5	14.2	7.2	0.7
8	0.91	36.0	23.5	14.2	7.2	1.9
9		36.0	23.5	14.2	7.2	
10		36.0	23.5	15.5	8.3	1.3
11	1.13	36.0	23.5	15.5	8.3	2.9
12		36.0	23.5	15.5	8.3	
13		36.0	23.5	15.5	9.1	2.5
14	1.27	36.0	23.5	15.5	9.1	1.8
15		36.0	23.5	15.5	9.1	
16		36.0	23.5	15.0	8.6	2.2
17	1.41	36.0	23.5	15.0	8.6	1.5
18		36.0	23.5	15.0	8.6	
19		36.0	23.5	15.2	8.1	2.1
20	1.56	36.0	23.5	15.2	8.1	1.3
21		36.0	23.5	15.2	8.1	
22		36.0	23.5	15.5	8.6	1.8
23	1.70	36.0	23.5	15.5	8.6	1.3
24		36.0	23.5	15.5	8.6	
25		36.0	23.5	16.1	9.9	2.8
26	1.84	36.0	23.5	16.1	9.9	2.4
27		36.0	23.5	16.1	9.9	

Let the lower frequency of two monochromatic waves used be $f^{(1)}$, the higher $f^{(2)}$, and two times these elementary frequencies $f^{(11)}$ and $f^{(22)}$ respectively. Then, because of the nonlinear interaction of 2nd order, it is expected that further two components frequencies of which are the summation and difference of $f^{(1)}$ and $f^{(2)}$, that is, $f^{(1+2)}$ and $f^{(2-1)}$ exist in addition to above mentioned four components. Let two elementary wave periods be $T^{(1)}$ and $T^{(2)}$. Then the following relationships are given⁶⁾.

$$\left. \begin{aligned} f^{(1)} &= 1/T^{(1)} = 5/(5 T^{(1)}), & f^{(22)} &= 2 f^{(2)} = 14/(5 T^{(1)}), \\ f^{(2)} &= 1/T^{(2)} = 1/(T^{(1)}/\sqrt{2}) = 7/(5 T^{(1)}), & f^{(1+2)} &= f^{(1)} + f^{(2)} = 12/(5 T^{(1)}), \\ f^{(11)} &= 2 f^{(1)} = 10/(5 T^{(1)}), & f^{(2-1)} &= f^{(2)} - f^{(1)} = 2/(5 T^{(1)}). \end{aligned} \right\} \dots \dots \dots (1)$$

c) Examples of experimental results

Fourier analyses were carried out and the spectra of the component wave height were obtained for all measuring points of all experimental cases in Table 1. A computer KDC-II of Kyoto University Computation Center was used for the Fourier analysis. Fig.2 shows the component wave height spectra of run No.6 (composite waves) $H^{()}$ in the uniform depth region and at the breaking point (Gauge No.4). The unit of abscissa is $1/(5T^{(1)})$. As seen in Eq.(1), 2, 5, 7, 10, 12 and 14 of the abscissa correspond to $f^{(2-1)}$, $f^{(1)}$, $f^{(2)}$, $f^{(11)}$, $f^{(1+2)}$ and $f^{(22)}$ respectively. In the uniform depth region, as shown in the figure (1), all of four secondary components $H^{(11)}$, $H^{(22)}$, $H^{(1+2)}$ and $H^{(2-1)}$ are considerably smaller than two elementary components $H^{(1)}$ and $H^{(2)}$. On the other hand, at the breaking point, as seen in the figure (2), all of four secondary components grow up and are not negligible.

RANDOM WAVES

a) Experimental apparatus

The same wave tank as in the experiments of composite waves was used. In this case, an electro-hydraulic random wave generator (see Photo.2) was used. This random wave generator is installed at the opposite tank end of the composite wave generator. Several kinds of input signal are available in this generator. In this experiment, the modified random noises passing through 15 bandpass filters having the center frequencies ranged from 0.2Hz to 5.0Hz were utilized.

As seen in Fig.3, a uniform sloping beach was installed in the middle part of the tank as in the experiments of composite waves. This beach was made of aluminium plates, and the slope of the beach was 1/20. Its length was 9.4m and the height of the beach tail was 47cm. The water depth in the uniform depth region was kept constant (47cm) to make negligible the effect of wave reflection as in the case of composite waves.

In the experiments, four wave gauges and the magnetic tape recorder were also used. The breaking point of random waves varies with time and could not be determined. So the depths of three measuring points on the beach were fixed as 31cm, 20cm and 10.5cm respectively during the experiments independently of the breaking point.

b) Procedure of experiment and analysis

At first, the experiments of random waves having power spectral density distribution of narrow band were carried out. Such random waves were considered to correspond to the monochromatic waves and generated by using one of the bandpass filters. Secondly, the experiments of random waves having two main peaks in power

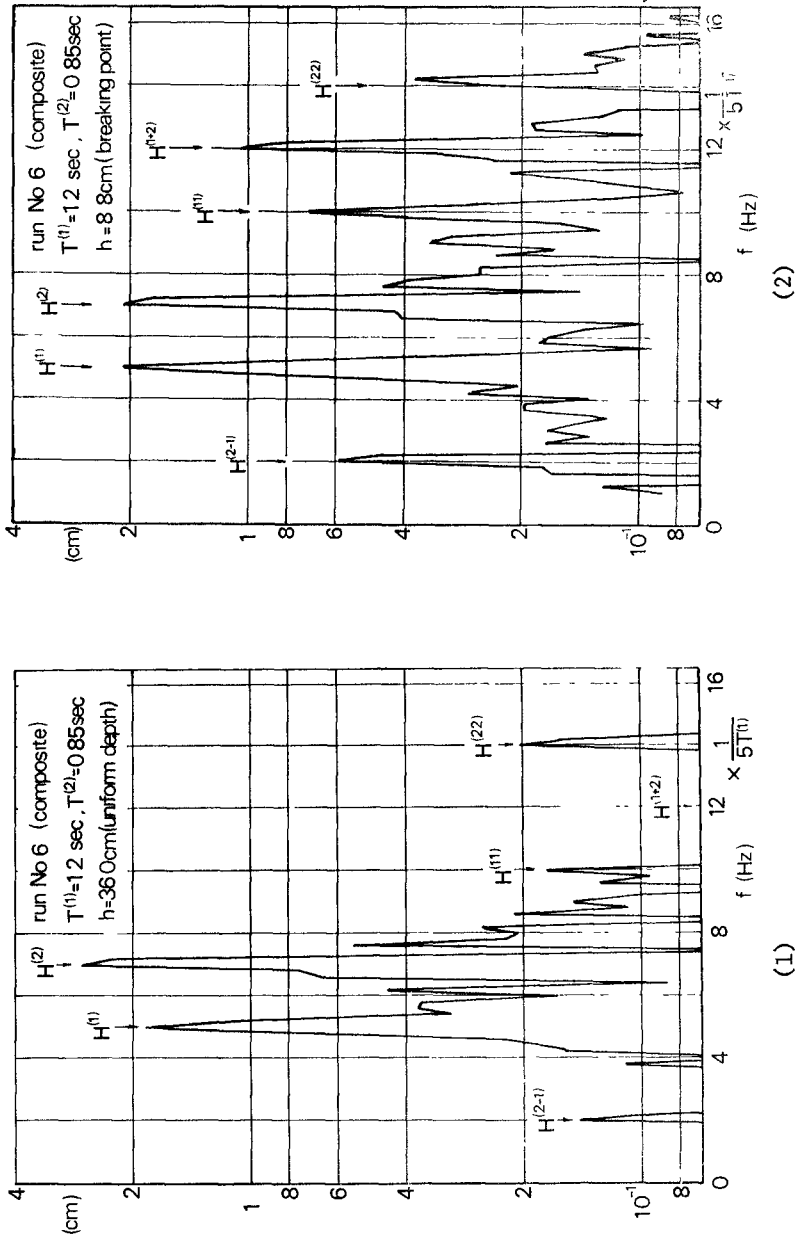


Fig. 2 Example of component wave height spectra of composite waves



Photo.2 Random wave generator

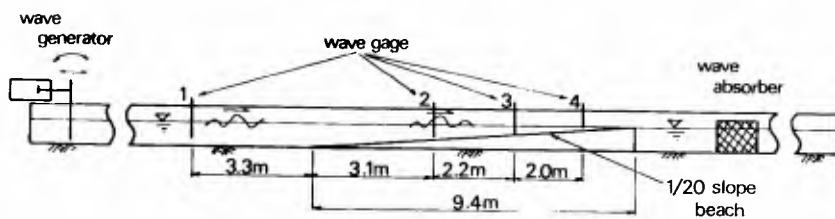


Fig.3 Experimental apparatus (random waves)

spectral density distribution were carried out. These random waves were considered to correspond to the composite waves having two elementary components and generated by using two of the bandpass filters. As in the case of composite waves, the analog data in the magnetic tape recorder were converted into the digital data with the time increment of 0.08sec by the A-D convertor for the numerical computations. The experimental conditions are shown in Table 2.

Power spectral densities were calculated for all records of water level variation by Blackman-Tukey's method, in which the number of data was 2000, the number of maximum lag 200, and the degree of freedom about 20. Also KDC-II of Kyoto University Computation Center was used for the numerical computations.

c) Examples of experimental results

Fig. 4 shows the power spectral density distributions at four measuring points in Run No.4. In the uniform depth region(full line), the main peak of power spectrum exists at about 0.8Hz and the subpeak at about two times the main peak frequency(1.6Hz). As the water depth decreases, the power of main peak decreases after the initial increase and the power of subpeak increases after the initial decrease. At the shallowest measuring point(chain line), the power of subpeak grows up to more than 30% of that of main peak.

CHANGES OF ELEMENTARY AND SECONDARY COMPONENT WAVE HEIGHTS OF COMPOSITE WAVES

a) Change of elementary component wave height of finite amplitude waves in shoaling water

In Fig. 5, the solid and chain curves are the shoaling curves of finite and small amplitude waves respectively. As indicated in the figure, solid curves of the right hand side group are calculated by using the energy flux of the third order approximation of Stokes waves and those of the left hand side group calculated by using the second approximation of hyperbolic waves⁷⁾. It is assumed that the wave height change of waves of a given deep-water wave steepness obeys the rule shown by these shoaling curves and the wave profile is represented by the summation of the elementary component, the component of two times the elementary frequency(the second harmonics) and the component of three times the elementary frequency(the third harmonics) as the third order approximation of Stokes waves⁸⁾.

The wave profile of 3rd order approximation of Stokes waves is given by Eq.

(2) where L is the wave length, $\theta=2\pi x/L-2\pi t/T$, x the coordinate in the direction

$$\eta/L = A_1 \cdot \cos \theta + A_2 \cdot \cos 2\theta + A_3 \cdot \cos 3\theta \quad \dots \dots \dots (2)$$

of wave propagation and T the wave period. Let the elementary component wave height be $H^{(1)}$ and the deep-water wave height H_0 . Then the ratio $H^{(1)}/H_0$ is written as

$$H^{(1)}/H_0 = 2A_1 \cdot (H_0/L_0)^{-1} \cdot (h/L)^{-1} \cdot h/L_0, \quad \dots \dots \dots (3)$$

where L_0 is the deep-water wave length and h the water depth. A_1 is given by

$$A_1 = a/L, \quad H/L = 2 \cdot a/L + 2\pi^2(a/L)^3 \cdot f_3, \quad \dots \dots \dots (4)$$

$$f_3(h/L) = \frac{3}{16} \cdot \left\{ 8 \left(\cosh \frac{2\pi h}{L} \right)^4 + 1 \right\} / \left(\sinh \frac{2\pi h}{L} \right)^6 \quad \dots \dots \dots (5)$$

Since the value of h/L is determined by giving the values of H_0/L_0 , $H^{(1)}/H_0$ can

Table 2 Experimental conditions (random waves)

Run No.	Filter frequency	Water depth			
		Gauge No.1 uniform depth	No.2	No.3	No.4
	f (Hz)	h_1 (cm)	h_2 (cm)	h_3 (cm)	h_4 (cm)
1	1.28	46.7	31.0	19.9	10.3
2	1.25	46.8	31.1	20.0	10.4
3	1.00	46.8	31.1	20.0	10.4
4	0.80	46.7	31.0	19.9	10.3
5	0.50	46.7	31.0	19.9	10.3
6	1.60, 1.00	46.7	31.0	19.9	10.3
7	1.00, 0.63	46.7	31.0	19.9	10.3
8	0.80, 0.50	46.7	31.0	19.9	10.3
9	0.63, 0.40	46.7	31.0	19.9	10.3

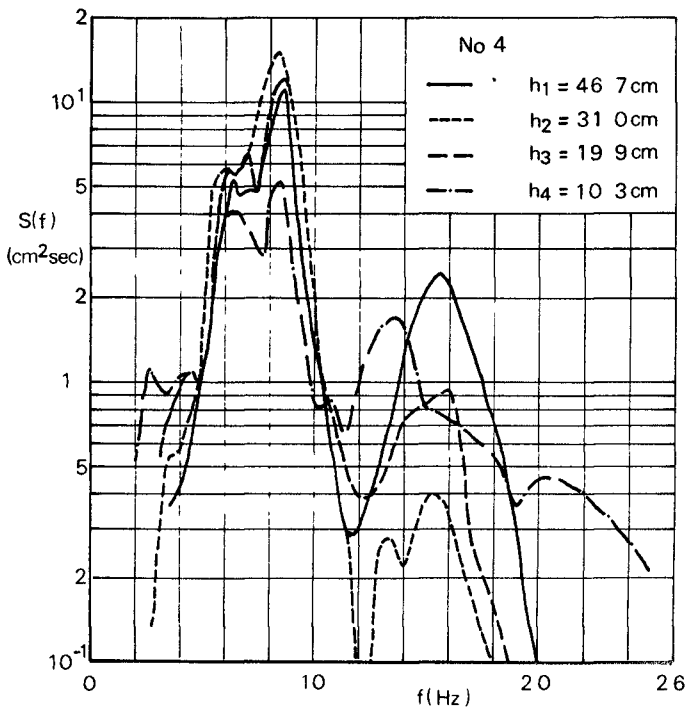


Fig.4 Example of power spectral densities of random waves

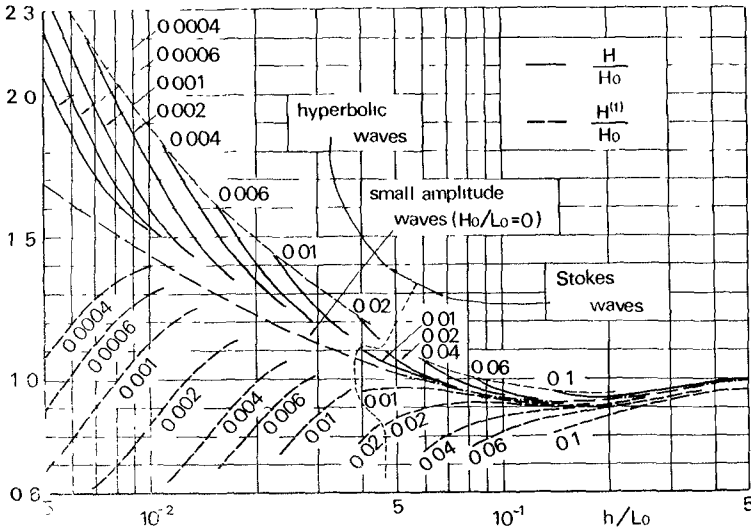
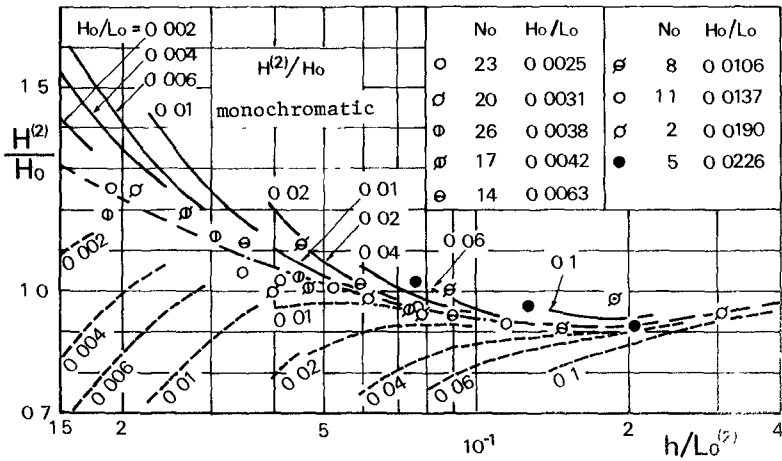


Fig.5 Change of elementary component wave height based on shoaling theory of finite amplitude waves



(1)

Fig.6 Changes of elementary component wave heights of monochromatic and composite waves

be obtained by using Eq.s (4), (5) and (3). The broken curves in Fig.5 show the changes of $H^{(1)}/H_0$ calculated in this manner. It should be noticed that while the wave height increases in shoaling water the elementary component wave height decreases.

b) Effects of internal viscosity and boundary friction

Before the change of elementary component wave height is discussed, the effects of internal viscosity and boundary friction were examined. In order to estimate the effect of bottom friction, the theoretical result for wave height change on a uniform sloping beach derived by Tsuchiya and Inoue³⁾ was utilized, which takes into account the effect of bottom friction. It was found that the effect of bottom friction on the wave height reduction is about 1%. Considering that the effects of internal viscosity and sidewall friction are the same order of magnitude as that of bottom friction, the effects of internal viscosity and boundary friction are expected to be the same order of magnitude as the experimental errors and therefore negligible.

c) Changes of elementary component wave heights of monochromatic and composite waves

Changes of two elementary component wave heights $H^{(1)}$ and $H^{(2)}$ are compared with the theoretical curves in Fig.5. The value of deep-water wave length is calculated by using the relationship of small amplitude waves $L_0 = gT^2/(2\pi)$ from two elementary wave periods $T^{(1)}$ and $T^{(2)}$. Unfortunately, the water leakage through the gap between the beach plate and the tank bottom near the toe of beach was inevitable. Therefore, it was expected that the some wave energy loss existed between two measurement points in the uniform depth region and on the beach. After all, the data in the uniform depth were abandoned and the deep-water wave height H_0 was determined by assuming that both values of $H^{(1)}/H_0$ and $H^{(2)}/H_0$ at the water depth h_2 agree with the theoretical values of shoaling curve of small amplitude waves (the chain line in Fig.5).

Fig.6 (1)~(3) show the experimental results and the theoretical curves in Fig.5. Fig.6 (1) shows the results of the elementary component $H^{(2)}$ of the monochromatic waves of shorter period, Fig.6 (2) the elementary component of longer period $H^{(1)}$ of the composite waves, and Fig.6 (3) the elementary component of shorter period $H^{(2)}$ of the composite waves. As seen in the figure (1), the elementary component wave height $H^{(2)}$ of the monochromatic waves of the shorter period does not show such decrease that the theory predicts. The experimental values scatter around the shoaling curve of small amplitude waves. The experimental results of the elementary component wave height $H^{(1)}$ of the monochromatic waves of longer period are not presented here, but those show the same behaviour.

On the other hand, in Fig.6 (2), the elementary component wave heights $H^{(1)}$ of longer period of the composite waves, except for Runs No.6 and No.9, depart from the curve by the small amplitude wave theory and decrease. However, as seen from the experimental values of deep-water wave steepness, the rates of decrease in experimental values are smaller than those in theoretical values. In Fig.6 (3), the elementary component wave heights $H^{(2)}$ of shorter period of composite waves decrease more rapidly than the theoretical curves. In any way, it is interesting that the decrease in elementary component wave height of composite waves in shoaling water is explained qualitatively by the theory of elementary component wave height change of finite amplitude waves in shoaling water.

d) Changes of secondary component wave heights of monochromatic and composite waves

The linear composite waves having two elementary components are represented

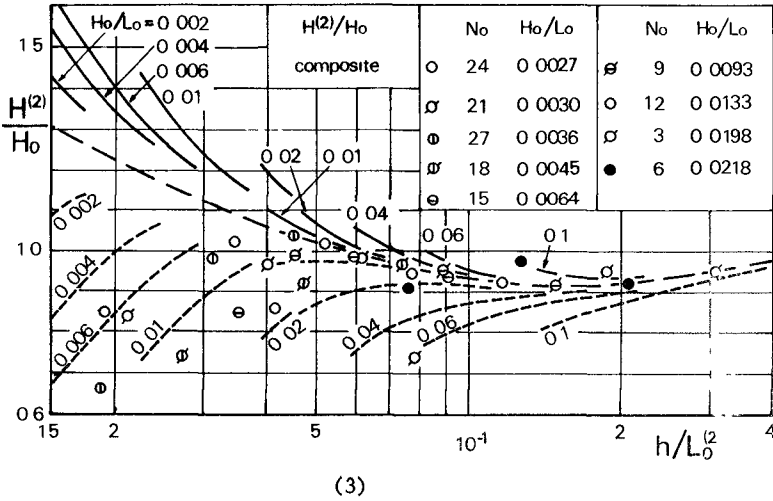
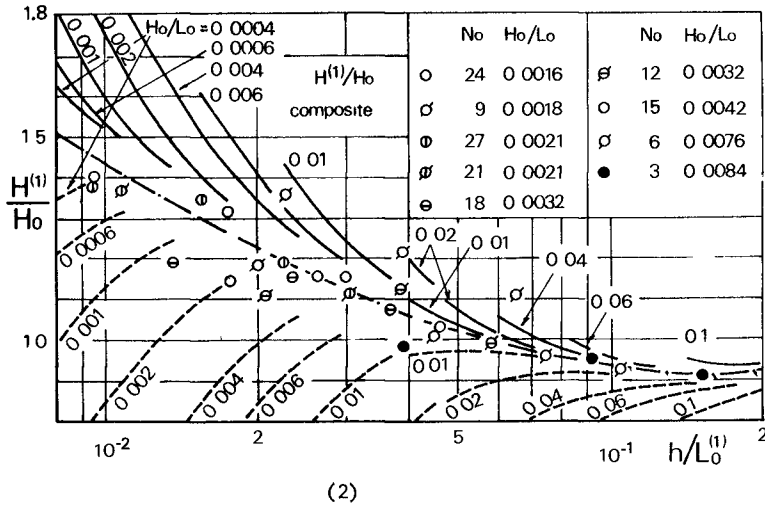


Fig. 6 Changes of elementary component wave heights of monochromatic and composite waves

as follows :

$$\eta = a_1 \cos k_1(x - c_1 t) + a_2 \cos k_2(x - c_2 t) \quad (6)$$

where the suffix means the elementary component, k is the wave number and c the wave celerity. c_1 and c_2 are related to k_1 and k_2 respectively with the small amplitude wave theory. Let two elementary component wave heights be H_1 and H_2 . Then $H_1 = 2a_1$ and $H_2 = 2a_2$. Four secondary components are produced due to the nonlinear interaction of the second order. Hamada⁶ derived the following relations of these four secondary component wave heights H_{1+2} , H_{2+2} , H_{1+2} and H_{2-1} theoretically:

$$H_{11} = \frac{2}{g} \left\{ 2 k_1 c_1 B_{11} \coth 2 k_1 h + \frac{1}{2} b_1^2 k_1^2 - \frac{1}{4} b_1^2 k_1^2 (\coth^2 k_1 h - 1) \right\} \quad (7)$$

$$H_{22} = \frac{2}{g} \left\{ 2 k_2 c_2 B_{22} \coth 2 k_2 h + \frac{1}{2} b_2^2 k_2^2 - \frac{1}{4} b_2^2 k_2^2 (\coth^2 k_2 h - 1) \right\} \quad (8)$$

$$H_{1+2} = \frac{2}{g} \left\{ (c_1 k_1 + c_2 k_2) B_{1+2} \coth (k_1 + k_2) h + \frac{1}{2} (k_1^2 c_1 b_1 a_2 + k_2^2 c_2 b_2 a_1) - \frac{1}{2} b_1 b_2 k_1 k_2 (\coth k_1 h \coth k_2 h - 1) \right\} \quad (9)$$

$$H_{2-1} = \frac{2}{g} \left\{ (c_2 k_2 - c_1 k_1) B_{2-1} \coth (k_2 - k_1) h + \frac{1}{2} (k_1^2 c_1 b_1 a_2 + k_2^2 c_2 b_2 a_1) - \frac{1}{2} b_1 b_2 k_1 k_2 (\coth k_1 h \coth k_2 h + 1) \right\} \quad (10)$$

where $b_1 = a_1 \times c_1$, $b_2 = a_2 \times c_2$,

$$B_{11} = \frac{-\frac{3}{2} b_1^2 k_1^3 c_1 (\coth^2 k_1 h - 1)}{-4 k_1^3 c_1^2 \coth 2 k_1 h + 2 k_1 g} \quad (11)$$

$$B_{22} = \frac{-\frac{3}{2} b_2^2 k_2^3 c_2 (\coth^2 k_2 h - 1)}{-4 k_2^3 c_2^2 \coth 2 k_2 h + 2 k_2 g} \quad (12)$$

$$B_{1+2} = \frac{b_1 b_2 k_1 k_2 (c_1 k_1 + c_2 k_2) (1 - \coth k_1 h \coth k_2 h) - \frac{1}{2} b_1 k_1^3 a_2 c_1^2 (\coth^2 k_1 h - 1) - \frac{1}{2} b_2 k_2^3 a_1 c_2^2 (\coth^2 k_2 h - 1)}{-(c_1 k_1 + c_2 k_2)^2 \coth (k_1 + k_2) h + (k_1 + k_2) g} \quad (13)$$

$$B_{2-1} = \frac{b_1 b_2 k_1 k_2 (c_2 k_2 - c_1 k_1) (1 + \coth k_1 h \coth k_2 h) - \frac{1}{2} b_1 k_1^3 a_2 c_1^2 (\coth^2 k_1 h - 1) + \frac{1}{2} b_2 k_2^3 a_1 c_2^2 (\coth^2 k_2 h - 1)}{-(c_1 k_1 - c_2 k_2)^2 \coth (k_1 - k_2) h + (k_1 - k_2) g} \quad (14)$$

In order to compare the experimental values of secondary component wave heights with Hamada's theoretical values, the composite waves at uniform depths h_i ($i=1 \sim 4$), which correspond to the water depths at measuring points, are considered. In this case, the experimental values $H^{(1)}$, $H^{(2)}$, $T^{(1)}$ and $T^{(2)}$ are adopted as H_1 , H_2 and two wave periods. Fig. 7 (1)~(4) show the comparisons of experimental values of four secondary component wave heights with theoretical ones calculated in such a manner. Fig. 7 (1) and (2) show the results of Run No.s 1~3 which form one group. Fig. 7 (3) and (4) show the results of Run No.s 16~18 which form the other group. The values of L_0 were calculated by using the relationship of small amplitude waves and the frequencies of secondary components. As seen in the figures, the behaviours of increase in the experimental values of four secondary component wave heights shown with thick lines are explained qualitatively by the theoretical lines shown with thin lines.

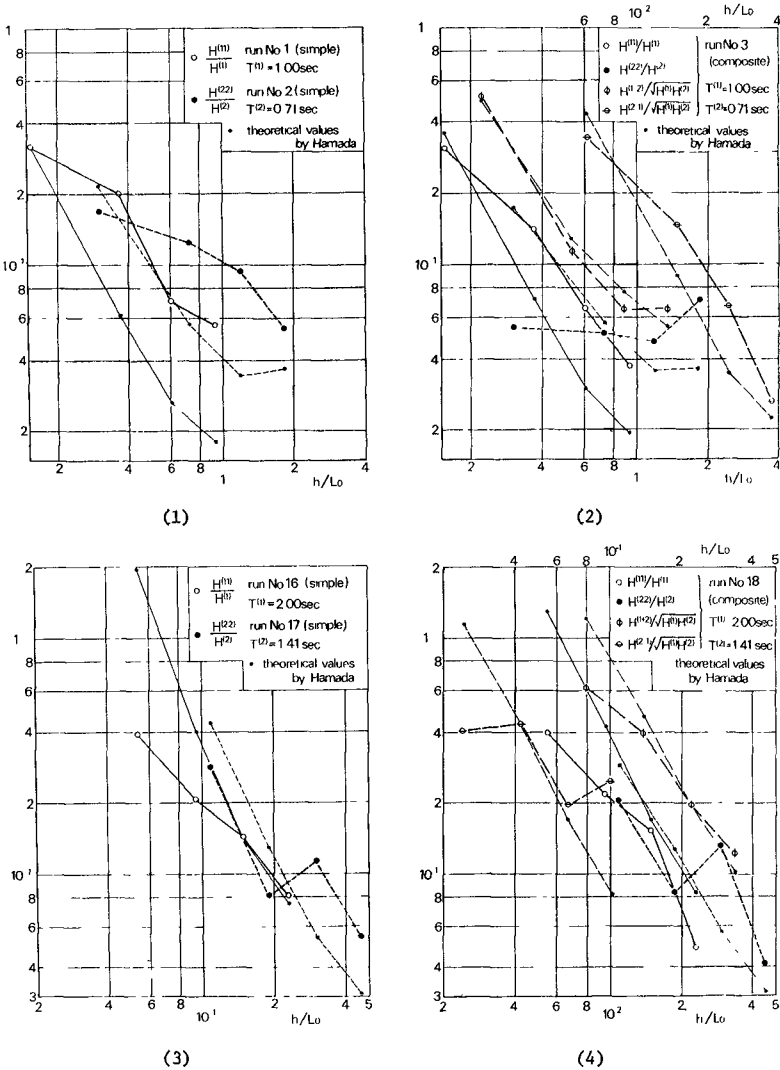


Fig.7 Changes of secondary component wave heights of monochromatic and composite waves

CHANGES OF ELEMENTARY AND SECONDARY PEAK POWERS OF RANDOM WAVES

a) Changes of elementary peak power of random waves having one main peak

Fig. 4 shows the change of power spectra of Run No 4 in the case of random waves having one predominant frequency in power spectra. Although the predominant frequency changes slightly at four measuring points, it is denoted as $f^{(1)}$ to correspond to the elementary component frequency of the composite waves. The subpeak appears at about two times the value of $f^{(1)}$ which is denoted as $f^{(11)}$. The power spectral densities $S(f^{(1)})$ and $S(f^{(11)})$ at these two frequencies $f^{(1)}$ and $f^{(11)}$ are called the elementary and secondary powers respectively. The changes of values of $\sqrt{S(f^{(1)})}$ in shoaling water are discussed in comparison with the theoretical curves of elementary component wave height change of finite amplitude waves shown with the broken line in Fig. 5

The values of L_0 were calculated by using the relationship of small amplitude waves, and the values of $f^{(1)}$. The power spectral density $S_0(f^{(1)})$ at the frequency $f^{(1)}$ in deep water was assumed as the quantity corresponding to the deep-water wave height H_0 . This quantity was calculated by assuming that the value of $\sqrt{S(f^{(1)})}/S_0(f^{(1)})$ agrees with that of the shoaling curve of small amplitude waves (chain line) in the uniform depth region.

Fig. 8 (1) shows the experimental results of $\sqrt{S(f^{(1)})}/S_0(f^{(1)})$ of random waves having one main peak in comparison with the theoretical curves of elementary component wave height change of finite amplitude waves. As seen in the figure, the experimental values scatter considerably. The experimental values of Run No.s 4 and 3 are much larger than the values of theoretical curves (broken line). However, the experimental values of Run No.s 5, 2 and 1 show the behaviour of decrease as well as the theoretical curves. The parameter of theoretical curves is the deep-water wave steepness H_0/L_0 . For the purpose of comparison, a dimensional quantity $f^{(1)2} S_0(f^{(1)})^{1/2}$ is calculated as the quantity corresponding to H_0/L_0 of monochromatic waves. However, in the case of random waves having one main peak, it is difficult to find the relationship between this dimensional parameter and the change of elementary peak power.

In Fig. 8 (1), the experimental values by Sawaragi and Tabata¹⁰⁾ are also shown. The decrease of elementary peak power is explained qualitatively by the theoretical curves.

b) Changes of elementary peak power of random waves having two main peaks

Fig 8 (2) shows the experimental values of two elementary peak powers in the case of random waves of Run No s 6~9. In the figure, $S(f^{(1)})$ and $S(f^{(2)})$ mean the peak powers of the lower and higher frequencies respectively. In this case, the experimental values of all runs decrease in the same manner as the theoretical curves. Further, the larger the value of the parameter $f^{(1)2} S_0(f^{(1)})^{1/2}$ corresponding to the deep-water wave steepness, the more rapidly the experimental value of power decreases. As in the case of composite waves, it is interesting that the decrease of two elementary peak powers of random waves is explained qualitatively by the theoretical curves of elementary component wave height change of finite amplitude waves.

c) Changes of secondary peak powers of random waves

The case shown in Fig. 4 is of random waves having one main peak, and it is easy to detect the secondary peak in the power spectral density distribution. However, in the random waves having two main peaks Run No.s 6~9, four secondary peaks must exist and it is difficult to detect them in the distribution. Therefore, only the secondary peak powers of random waves having one main peak are discussed

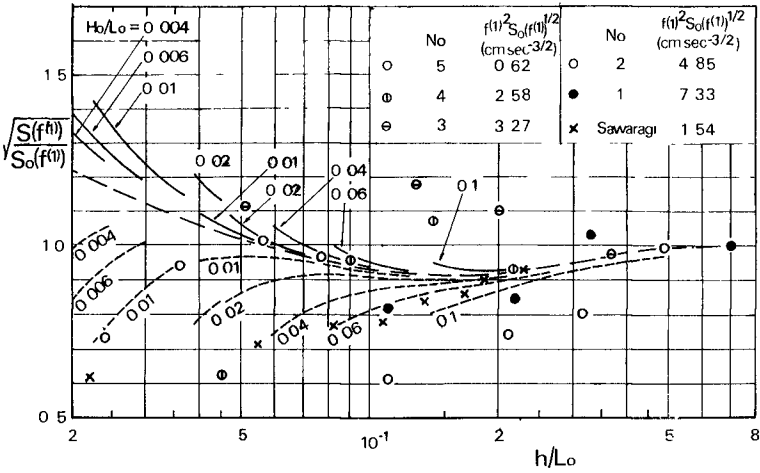


Fig.8 (1) Changes of elementary component powers of random waves (one main peak)

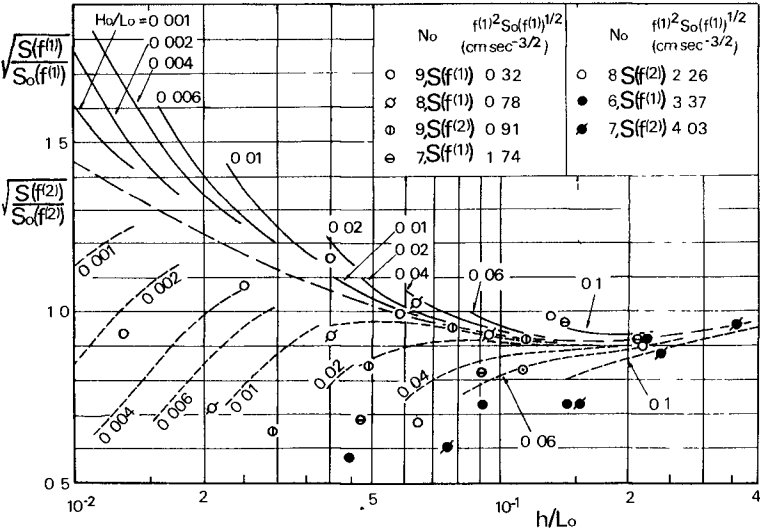


Fig.8 (2) Changes of elementary component powers of random waves (two main peaks)

here.

Let the power spectral density of linear random waves in uniform depth be $S_1(\omega)$, in which the spectrum is two-sided and ω is the angular frequency $2\pi f$. Hamada⁶ derived the secondary power spectral density $S_2(\lambda)$ due to nonlinear interaction of 2nd order in uniform depth as follows:

$$S_2(\lambda) = \int_{-\infty}^{\infty} K(\omega, \lambda) \cdot S_1(\lambda - \omega) \cdot S_1(\omega) d\omega, \quad \dots \dots \dots (15)$$

where $K(\omega, \lambda)$ is given as

$$K(\omega, \lambda) = \frac{1}{4} \left[\frac{g k k(\lambda - \omega)}{\omega(\lambda - \omega)} + \frac{\omega(\lambda - \omega)}{g} - \frac{\lambda^2}{g} + \lambda^2 \left\{ \frac{g(\lambda - \omega)k^2 + g\omega k^2(\lambda - \omega)}{\omega(\lambda - \omega)\lambda} \right. \right. \\ \left. \left. + \frac{2g k k(\lambda - \omega)}{\omega(\lambda - \omega)} + \frac{\omega(\lambda - \omega)}{g} - \frac{\lambda^2}{g} \right\} / \{g[k + k(\lambda - \omega)] \cdot \tanh[k + k(\lambda - \omega)]k - \lambda^2\} \right], \quad \dots \dots (16)$$

and k and $k(\lambda - \omega)$ are wave numbers which are functions of ω and $\lambda - \omega$ respectively.

In order to compare experimental values with the theoretical ones above mentioned, the random waves in the same uniform depth as the water depth at each measuring point were assumed. As the linear power spectral density $S_1(\omega)$, the distribution consisting of an elementary peak and the base shown by a chain line in Fig.9 is adopted. The peak expressed by a broken line is the theoretical secondary peak power spectral density calculated by Eq.(15). Fig.10 shows the changes of secondary peak powers $S(f^{(11)})$ of Run No.s 2~5 in comparison with the theoretical secondary peak powers calculated in such a manner. L_0 in the abscissa was the calculated deep-water wave length of small amplitude waves by using the frequency $f^{(11)}$. As seen in the figure, the experimental values of secondary peak powers $S(f^{(11)})$ increase, in some cases after the initial decrease with decrease in the water depth, and are not negligible compared with the elementary peak powers. This experimental behaviour is explained qualitatively by Hamada's theory.

CONCLUSIONS

In this investigation, the mechanism of transformation of irregular waves (composite and random waves) in shoaling water was discussed experimentally. The damping due to internal viscosity and boundary friction was found to be negligible because it is of the same order of magnitude as the experimental error.

The elementary component wave heights of composite waves consisting of two elementary components and the elementary peak powers of random waves having one or two main peaks decrease, in some cases after the initial increase, with decrease in the water depth. This was explained by the theory of elementary component wave height change of finite amplitude waves in shoaling water derived from the shoaling curves of finite amplitude waves.

The four secondary component wave heights of composite waves consisting of two elementary components and the secondary peak powers of random waves having one main peak increase, in some cases after the initial decrease with decrease in the water depth, and become to be not negligible compared with the elementary component wave heights and powers. This was explained by the theory of nonlinear interaction of 2nd order of composite and random waves in uniform depth.

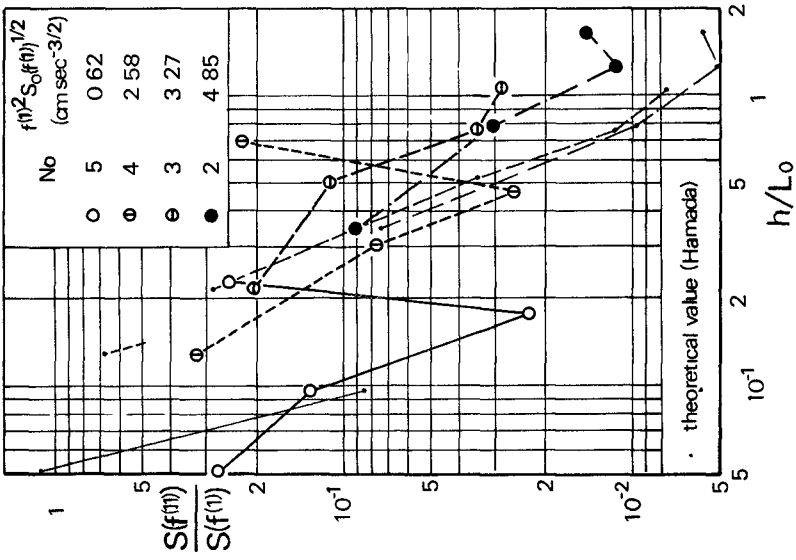


Fig. 10 Changes of secondary component powers of random waves

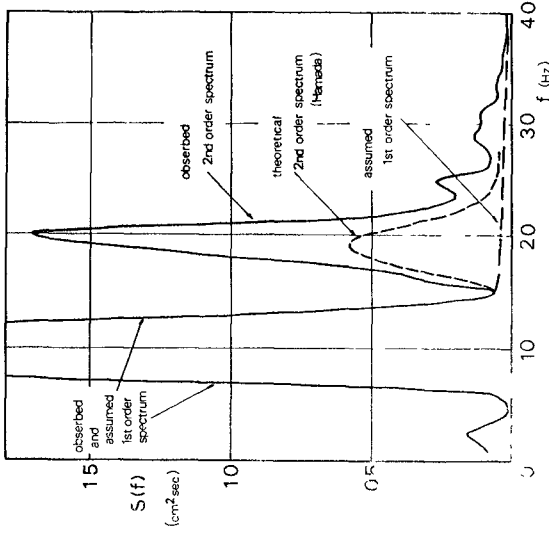


Fig. 9 Theoretical distribution of secondary component power of random waves

ACKNOWLEDGEMENTS

The authors wish to express their gratitudes to Messrs. I. Sakai and T. Morita for their assistances through the experiment and data analysis. This work was partly supported by Scientific Research Funds from the Ministry of Education

REFERENCES

- 1) Bretschneider, C. L. : Modification of wave spectra on the continental shelf and in the surf zone, Proc. 8th Conf. Coastal Engineering, pp.17-33, 1963.
- 2) Tang, F. L. W. and S. H. Ou : Researches on the deformation of wave spectra in intermediate water area by calculation, Proc. 13th Conf. Coastal Engineering, pp.271-288, 1973.
- 3) Hasselmann, K. Weak Interaction Theory of Ocean Waves, Basic Developments in Fluid Dynamics, Vol.2, pp.117-182, Academic Press, 1968.
- 4) Mitsuyasu, H. : A note on the nonlinear energy transfer in the spectrum of wind-generated waves, Rep. Res. Inst. Appl. Mech., Kyushu Univ., Vol.XVI, No.54, pp.251-264, 1968
- 5) Iwagaki, Y., Y. Tsuchiya and A. Ishida : A generator of irregular waves and analysis of generated waves, Proc. 13th Cong. International Association for Hydraulic Research, Vol.5-1, pp.289-292, 1969
- 6) Hamada, T. : The secondary interactions of surface waves, Rep. Port and Harbour Res. Inst. No.10, 1965
- 7) Iwagaki, Y. : Hyperbolic waves and their shoaling, Proc. 11th Conf. Coastal Engineering, pp.124-144, 1969.
- 8) Skjelbreia, L. : Gravity Waves, Stokes' Third Order Approximation, Table of Functions, Council on Wave Research, The Engineering Foundation, 1959.
- 9) Tsuchiya, Y. and M. Inoue Basic study on wave damping due to bottom friction (1), Proc. 8th Conf. Coastal Engineering in Japan, pp.19-24, 1961(in Japanese).
- 10) Sawaragi, T. and T. Tabata : Transformation of irregular waves in decay area, Proc. 19th Conf. Coastal Engineering in Japan, pp 143-148, 1972(in Japanese).